



ELSEVIER

Physica C 288 (1997) 217–225

PHYSICA C

The van Hove scenario of high T_c superconductors: the effect of doping

J. Bouvier^{*}, J. Bok

Laboratoire de Physique du Solide, UPR 5 CNRS, ESPCI, 10 Rue Vauquelin, F-75231 Paris Cedex 05, France

Received 8 November 1996; revised 25 March 1997; accepted 19 May 1997

Abstract

We have previously established that the BCS gap equation, using an electron–phonon interaction term with weak screening and a 2D electronic band structure showing saddle points (vHs) at the points of the Brillouin zone, leads to an anisotropic gap Δ_k , the maximum gap Δ_{\max} is at point $\bar{M}(\pm\pi/a, 0)$ and $(0, \pm\pi/a)$ and the minimum gap Δ_{\min} at 45° , points $[\pm\pi/2a, \pm\pi/2a]$ of the Brillouin zone of a square lattice for the CuO_2 planes (we neglect the orthorhombic distortion). In this paper, we examine the consequences of doping, which varies the density of carriers in the CuO_2 planes, on the superconducting properties of the cuprates in the framework of this model. We use a rigid band model, the effect of doping is to vary the position of the Fermi level relative to the position of the singularity. We compute, the gap anisotropy $\Delta_{\max}/\Delta_{\min}$ and T_c , the density of state of quasiparticle excitations, the tunneling conductance and the specific heat. We compare our calculations to many different experiments, photoemission, tunneling spectroscopy, specific heat measurements and find an excellent agreement. We find an interesting new result; the anisotropy $\Delta_{\max}/\Delta_{\min}$ decreases with doping. This is observed in photoemission. © 1997 Elsevier Science B.V.

1. Introduction

The van Hove scenario explains many physical properties of high T_c superconductors [1–4] such as high T_c , anomalous isotope effect, gap anisotropy, etc. We also have shown [5] that T_c can vary in large proportions with the band width of the compound, this is due to the renormalization of the Coulomb repulsion μ in μ^* in wide band superconductors, but not in narrow band compounds. This explains that Sr_2RuO_4 has a very low T_c (~ 1 K) [6].

Recently we have shown that the existence of

saddle points in certain directions and weak screening of the electron–phonon interaction [2] explains the gap anisotropy. We then applied this result to the calculation of the density of states of quasiparticle excitations and of the $I(V)$ characteristics of tunnel junctions [7,8].

In this paper we investigate in details the effect of doping, that we treat in a rigid band model, i.e. the effect of overdoping is to displace the Fermi level from the singularity E_s . Our approach neglects magnetic fluctuations and is thus not applicable to underdoped material. But at optimum doping and for overdoped samples, the inelastic neutron scattering experiments [9] have shown that these magnetic excitations disappear.

In Section 2 we compute the critical temperature

^{*} Corresponding author. Fax: +33 1 40794425; e-mail: julien.bok@espci.fr

T_c and the maximum and minimum gaps Δ_{\max} and Δ_{\min} and hence the anisotropy as a function of doping and compare the results with the photoemission experiments.

In Sections 3 and 4 we use these results to compute the density of states of quasiparticle excitations and derive two important physical parameters that we can compare with experiments: the conductance of a tunnel junction and the electronic specific heat.

2. T_c and gap anisotropy as a function of doping

2.1. Model and basic equations

We use a rigid band model, the doping is represented by a shift $D = E_F - E_s$ of the Fermi level. This band structure is

$$\xi_k = -2t(\cos k_x a + \cos k_y a) - D. \quad (1)$$

The Fermi level is taken at $\xi_k = 0$. We use the same electron–phonon interaction potential as in our previous paper [2]

$$V_{kk'} = -\frac{|g_q|^2}{q^2 + q_0^2} < 0,$$

where $g(q)$ is the electron–phonon interaction matrix element for $\mathbf{q} = \mathbf{k}' - \mathbf{k}$ and q_0 is the inverse of the screening length. We use reduced units

$$X = k_x a, \quad Y = k_y a, \quad Q = qa, \quad u = \frac{\xi}{2t}, \quad \delta = \frac{D}{2t}.$$

We use the BCS equation for an anisotropic gap:

$$\Delta_k = -\frac{1}{2} \sum_{k'} \frac{V_{kk'} \Delta_{k'}}{\sqrt{\xi_{k'}^2 + \Delta_{k'}^2}}. \quad (2)$$

We compute Δ_k for two values of \mathbf{k} :

$$\begin{aligned} \Delta_A \text{ for } k_x a = \pi, \quad k_y a = 0, \\ \Delta_B \text{ for } k_x a = k_y a = \frac{\pi}{2}. \end{aligned} \quad (3)$$

We solve Eq. (2) by iteration using the same procedure as in Ref. [2]. We know from group theory considerations, that $V_{kk'}$ having a four-fold symmetry, the solution Δ_k has the same symmetry. We then

may use the angle Φ between the 0 axis and the \mathbf{k} vector as a variable and expand $\Delta(\Phi)$ in a Fourier series

$$\begin{aligned} \Delta(\Phi) = \Delta_0 + \Delta_1 \cos(4\Phi + \varphi_1) \\ + \Delta_2 \cos(8\Phi + \varphi_2) + \dots \end{aligned} \quad (4)$$

We know that $\varphi_1 = 0$, because the maximum gap is in the direction of the saddle points. We use the first two terms. The first step in the iteration is obtained by replacing Δ_k by $\Delta_{\text{av}} = \Delta_0$ in the integral of Eq. (2). We thus obtain, for the two computed values: $\Delta_A = \Delta_{\max} = \Delta_0 + \Delta_1$ and $\Delta_B = \Delta_{\min} = \Delta_0 - \Delta_1$, the following expression:

$$\begin{aligned} \Delta_{A,B}(T) = \lambda_{\text{eff}} \int_{u_{\min}}^{u_{\max}} \frac{\Delta_{\text{av}}(T)}{\sqrt{u^2 + u_{\text{av}}^2(T)}} \\ \times I_{(A,B)}(u) \tanh\left(\frac{\sqrt{u^2 + u_{\text{av}}^2(T)}}{k_B T/t}\right) du, \end{aligned} \quad (5)$$

$$\begin{aligned} I_{A,B}(u) = \int_0^{x'_0} \frac{dx'}{\{1 - [(\delta - u) - \cos x']^2\}^{1/2}} \\ \times \frac{(q_0 a)^2}{Q_{A,B}^2 + (q_0 a)^2}, \end{aligned} \quad (6)$$

where

$$u_{\min} = -\frac{\hbar \omega_c}{2t}, \quad u_{\max} = +\frac{\hbar \omega_c}{2t},$$

$$u_{\text{av}}(T) = \frac{\Delta_{\text{av}}(T)}{2t}, \quad x'_0 = a \cos\left(\frac{\delta - u}{2}\right),$$

where ω_c is the cut off frequency, for electron–phonon interaction, we take for ω_c a characteristic phonon frequency as discussed in Ref. [2].

We have taken three values of $\hbar \omega_c$, 60, 90 and 100 meV. Our results are presented in Table 1.

In the classical BCS theory, we have the relative variation $\Delta T_c/T_c = \Delta \omega_c/\omega_c$ for the same λ_{eff} . Then we can see in Table 1 that for $E_F - E_s = 0$, the discrepancy between this relation and our results, the isotopic effect is weak [1]. When E_F goes away from the singularity, $E_F - E_s \neq 0$, then the isotopic effect is strong and gets back to the BCS prediction.

For the following part of this work we will keep the value of $\hbar \omega_c = 60$ meV for the Bi2212 com-

Table 1
Isotopic effect on T_c within the van Hove model

$\hbar \omega_c$ (meV)	t (eV)	λ_{eff}	$q_0 a$	Δ_{av}	Δ_{max} (meV)	Δ_{min} (meV)	T_c (K)
For a shift of $E_F - E_s = 0$							
60	0.2	0.665	0.12	14.5	23.424	5.6031	90.75
90	0.2	0.665	0.12	17.582	27.735	7.4293	110.5
100	0.2	0.665	0.12	18.563	29.122	8.0037	116.6
For a shift of $E_F - E_s = 60$ meV							
60	0.2	0.665	0.12	4.7562	6.7686	2.7438	31.2
90	0.2	0.665	0.12	8.0242	11.581	4.4674	52.9
100	0.2	0.665	0.12	9.0961	13.156	5.0363	59.9

pound. This choice respects our approximation for $V_{kk'}$.

For the choice of t , the transfer integral comes from the photoemission experiments and is $t = 0.2$ eV as explained in Ref. [2].

$q_0 a$ is adjusted, it is the Thomas–Fermi approximation for small q .

λ_{eff} is adjusted so as to find the experimental value of Δ_{max} and Δ_{min} and we find a reasonable value of about 0.5. λ_{eff} is the equivalent of $\lambda - \mu^*$ in the isotropic 3D, BCS model.

In fact the values of $q_0 a$ and λ_{eff} must depend on the doping level D . This calculation will be done later.

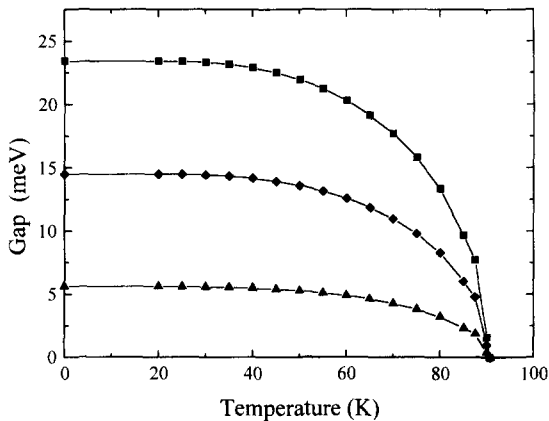


Fig. 1. Variation of the various gaps Δ_{max} , Δ_{min} and Δ_{av} versus the temperature, at the optimum doping, i.e. $D = E_F - E_s = 0$ in our model. With the following parameters $t = 0.2$ eV, $\hbar \omega_c = 60$ meV, $q_0 a = 0.12$, $\lambda_{\text{eff}} = 0.665$. The critical temperature found is $T_c = 90.75$ K. squares: Δ_{max} , diamonds: Δ_{av} , up triangles: Δ_{min} .

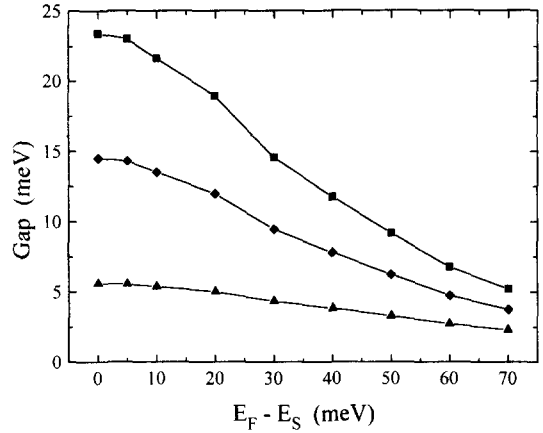


Fig. 2. Variation of the various gaps Δ_{max} , Δ_{min} , Δ_{av} versus the doping, $D = E_F - E_s$, at $T = 0$ K. squares: Δ_{max} , diamonds: Δ_{av} , up triangles: Δ_{min} .

2.2. Results

In Fig. 1, we present the variation of the various gaps Δ_{max} , Δ_{min} and Δ_{av} with temperature at optimum doping, i.e. for a density of holes of the order of 0.15 per CuO_2 plane. We take in that case $D = 0$ and we find $T_c = 91$ K and an anisotropy ratio $\alpha = \Delta_{\text{max}}/\Delta_{\text{min}} = 4.2$ and for the ratios of $2\Delta/k_B T_c$ the following values:

$$\frac{2\Delta_{\text{max}}}{k_B T_c} = 6.0, \quad \frac{2\Delta_{\text{av}}}{k_B T_c} = 3.7, \quad \frac{2\Delta_{\text{min}}}{k_B T_c} = 1.4.$$

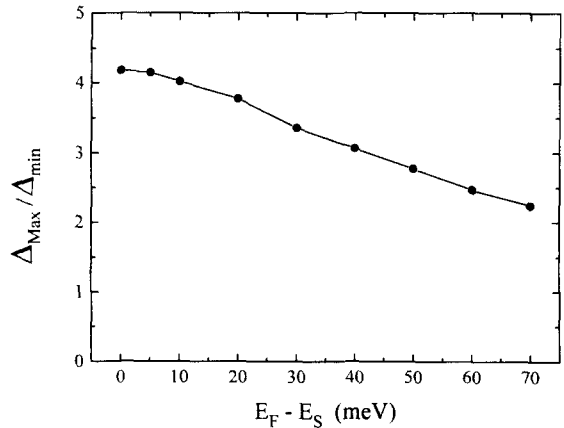


Fig. 3. Variation of the anisotropy ratio $\alpha = \Delta_{\text{max}}/\Delta_{\text{min}}$, versus the doping, $D = E_F - E_s$.

In Fig. 2 we present the same results, Δ_{\max} , Δ_{\min} , Δ_{av} as a function of $D = E_F - E_S$ (in meV).

In Fig. 3 we plot the variation of the anisotropy ratio $\alpha = \Delta_{\max}/\Delta_{\min}$ versus D . In Fig. 4(a) the critical temperature T_c versus D and in Fig. 5 the various ratios $2\Delta/k_B T_c$ versus D .

We observe of course that T_c and the gaps decrease with D or dx . The agreement with experiment [10] is very good (Fig. 4(b)). We obtain a new and interesting result which is the decrease of the anisotropy ratio α with doping. This is confirmed by recent results on photoemission [11,12] where a maximum gap ratio $2\Delta_{\max}/k_B T_c = 7$ is observed at optimum doping with $T_c = 83$ K and $2\Delta_{\max}/k_B T_c = 3$ for an overdoped sample with $T_c = 56$ K, with a

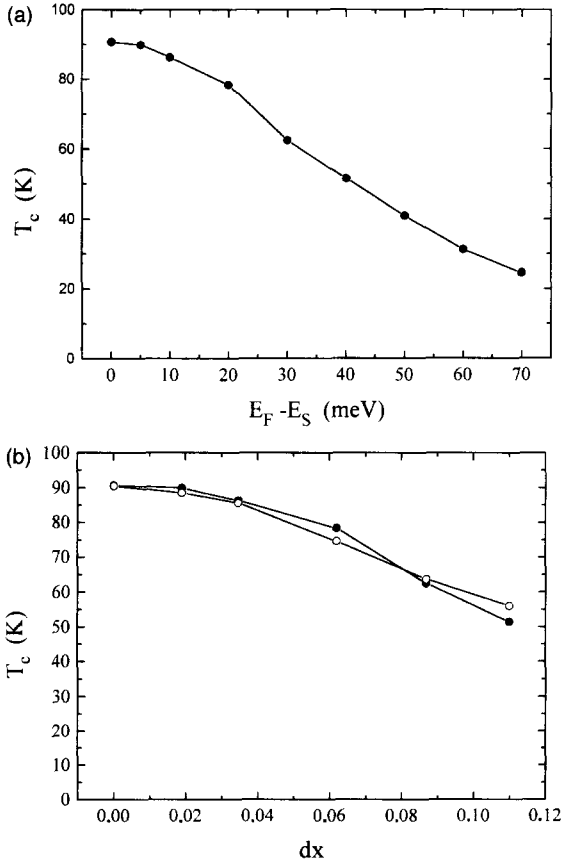


Fig. 4. (a) Variation of the critical temperature T_c versus the doping $D = E_F - E_S$. (b) Comparison of the variation of T_c versus the doping dx calculated in our model (filled circles) and the experimental results of Koike et al. [10] (open circles).

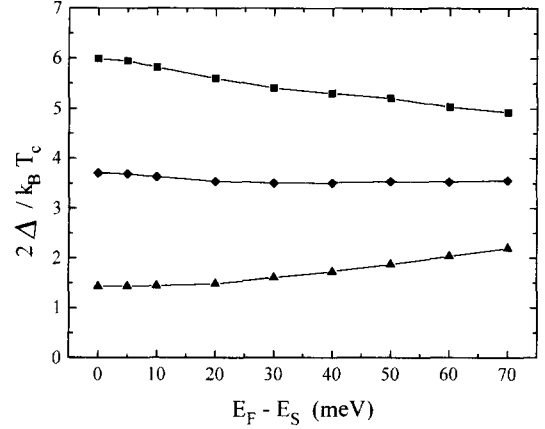


Fig. 5. Variation of the various ratios $2\Delta/k_B T_c$ versus the doping $D = E_F - E_S$. squares: $\Delta_{\max}/k_B T_c$, diamonds: $\Delta_{\text{av}}/k_B T_c$, up triangles: $\Delta_{\min}/k_B T_c$.

small gap $\Delta_{\min} = 0\text{--}2$ meV for both T_c , for a Bi2212 compound.

3. Density of states

The density of states, DOS, is computed using the formula:

$$n(\epsilon) = \frac{1}{2\pi^2} \frac{\partial A}{\partial \epsilon}, \quad (7)$$

where A is the area in k space between two curves of constant energy of the quasiparticle excitation ϵ_k given by:

$$\epsilon_k^2 = \xi_k^2 + \Delta_k^2, \quad (8)$$

where ϵ_k is the band structure (Eq. (1)). We use the same procedure and the same expression of Δ_k as in Refs. [7,8].

Fig. 6 represents the variation of the DOS as a function of ϵ for $T = 0$ K. This is similar to the conductance of a NIS junction. But for different values of $E_F - E_S$ we see a new maximum emerging, which is a signature of the van Hove singularity and a dip between that maximum and the peak at Δ_{\max} . This dip is seen experimentally in the STM tunneling experiments of Renner et al. [13]. The dip moves away from Δ_{\max} as the doping level, i.e. D increases. Fig. 7(a) shows the variation of the DOS

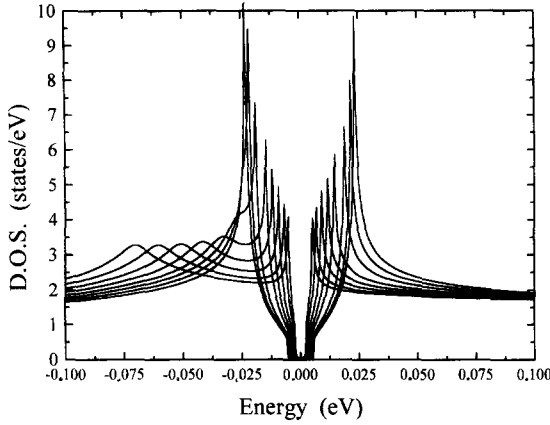


Fig. 6. Variation of the DOS versus the energy ϵ , for $T = 0$ K, that is similar at a NIS junction, for different values of the doping $D = E_F - E_s$, i.e. 0, 10, 20, 30, 40, 60 and 70 meV with $\Gamma = 0.1$ meV and $\Gamma' = 5$ meV in the model of Refs. [7,8].

as function of temperature for $D = 0$ and then for $D = 60$ meV (Fig. 7(b)).

For the calculation of the conductance, we use the following formula

$$\frac{dI}{dV} = CN_0 \int_{-\infty}^{+\infty} N_s(\epsilon) \left(-\frac{\partial f_{FD}}{\partial V}(\epsilon - V) \right) d\epsilon, \quad (9)$$

where f_{FD} is the usual Fermi–Dirac function; I and V are the current and voltage, C a constant proportional to $|T|^2$, the square of the barrier transmission, N_0 the DOS of the normal metal that we assume constant, and $N_s(\epsilon)$ the previously calculated DOS in the anisotropic superconductor. The tunneling into an anisotropic superconductor is given in more details in previous papers [7,8]. We shall now use the calculated DOS to evaluate the specific heat.

4. Specific heat

4.1. Theoretical calculation

The purpose of this section is to evaluate the influence of the vHs and the anisotropy of the gap on the specific heat calculated in the mean field BCS approximation, i.e. we do not take into account the fluctuations near the critical temperature T_c . There are a great number of experiments measuring C_s . To compare our calculations to experiments, we must

subtract the part due to fluctuations. These kinds of adjustment have been made by various authors by using the fact that thermodynamic fluctuations are symmetric about T_c and can be easily evaluated above T_c [14–17].

Also we do not take into account the magnetic fluctuations in low temperature, nor the pair-breaker which may exist in overdoped sample.

C_s is calculated using the classical formula in the BCS framework. The entropy of the excited quasi-particle is given by

$$S = -2k_B \sum_k (1 - f_k) \ln(1 - f_k) + (f_k \ln f_k), \quad (10)$$

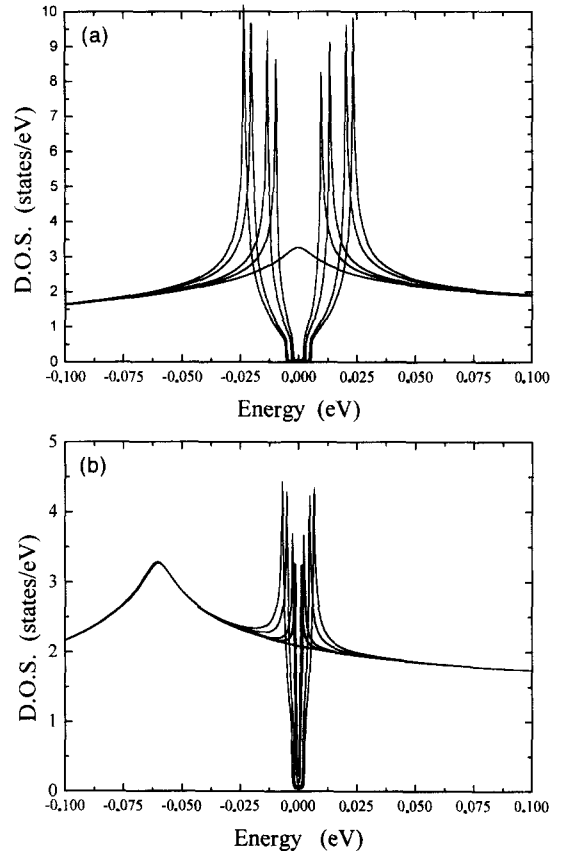


Fig. 7. (a) Variation of the DOS for different temperatures at the doping $D = E_F - E_s = 0$, with $\Gamma = 0.1$ meV and $\Gamma' = 5$ meV in the model of Refs. [7,8]. $T = 0, 60, 80, 85$ K and $T > T_c$. (b) Variation of the DOS for different temperatures at the doping $D = E_F - E_s = 60$ meV, with $\Gamma = 0.1$ meV and $\Gamma' = 5$ meV in the model of Refs. [7,8]. $T = 0, 25, 30, 30.8$ K and $T > T_c$.

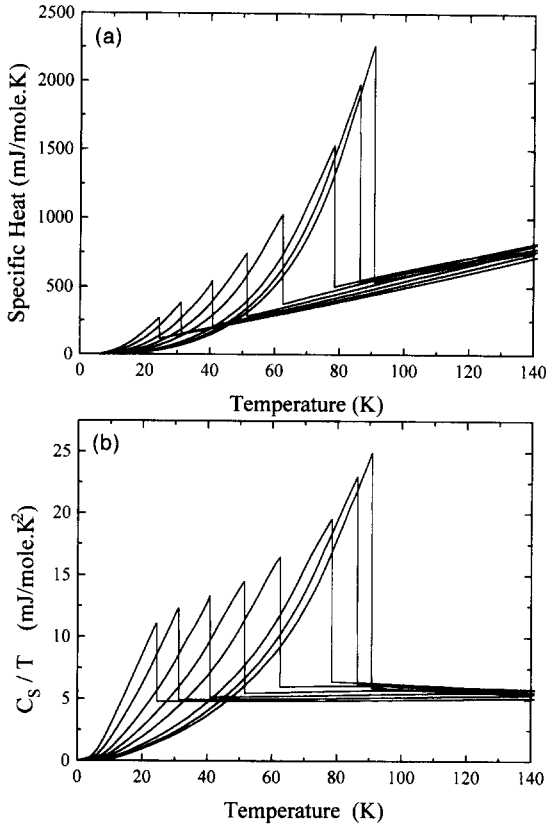


Fig. 8. (a) The calculated specific heat versus the temperature for different values of doping $D = E_F - E_s = 0, 10, 20, 30, 40, 50, 60$ and 70 meV. (b) The corresponding coefficient $\gamma_s = C_s/T$ for the same values of D as in (a).

f_k is the Fermi–Dirac distribution function and ϵ_k is given by Eq. (8). Then C_s is deduced from Eq. (10)

$$C_s = T \left. \frac{dS}{dT} \right|_V. \quad (11)$$

This gives

$$C_s(T) = \frac{2}{k_B T^2} \sum_k \frac{\exp(\epsilon_k/k_B T)}{[1 + \exp(\epsilon_k/k_B T)]^2} \epsilon_k^2 - \frac{1}{k_B T} \sum_k \frac{\exp(\epsilon_k/k_B T)}{[1 + \exp(\epsilon_k/k_B T)]^2} \frac{\partial \Delta_k^2(T)}{\partial T}. \quad (12)$$

We use the values of ϵ_k and Δ_k given by formulae (8) and (4) to evaluate the two integrals of Eq. (12) numerically.

The variation of $\Delta_{\max}(T, D)$ and $\Delta_{\min}(T, D)$ was

already done numerically in Figs. 1 and 2. Near T_c we have a very good agreement between the calculated values and the following analytical formula:

$$\Delta_{\max, \min} = \Delta_{\max, \min}(T=0) 1.7 \left(1 - \frac{T}{T_c} \right)^{1/2}.$$

We see that the slopes $\partial \Delta^2 / \partial T$ do not depend on doping which simplifies the calculation of the second integral of formula Eq. (12). The results are presented in Fig. 8(a),(b) where we plot C_s and C_s/T versus T for various doping levels D . We can make the following observations

(1) The jump in specific heat at $T = T_c$ varies with doping $\Delta C/C = (C_s - C_N)/C_N|_{T=T_c}$ is 3.2 for $D = 0$ and 1.48 for $D = 60$ meV compared to 1.41, the BCS value for a isotropic superconductor (*s*-wave) with a constant DOS, N_0 in the normal state. The high value of $\Delta C/C$ is essentially due to the vHs when it coincides with the Fermi level and the highest value of the gap Δ_k . With doping, the vHs moves away from E_F and $\Delta C/C$ decreases toward its BCS value of 1.41 (or 1.31, because we take 1.7 instead of 1.74 for the coefficient of the equation of the gaps near T_c), Fig. 9.

(2) There is also a difference in the specific heat C_N in the normal state. For a usual metal with a constant DOS, N_0 , $\gamma_N = C_N/T$ is constant and proportional to N_0 . Here we find $\gamma_N = a \ln(1/T) + b$ for $0 \leq D \leq 30$ meV where a and b are constant. For $D = 0$ this behaviour has already been predicted

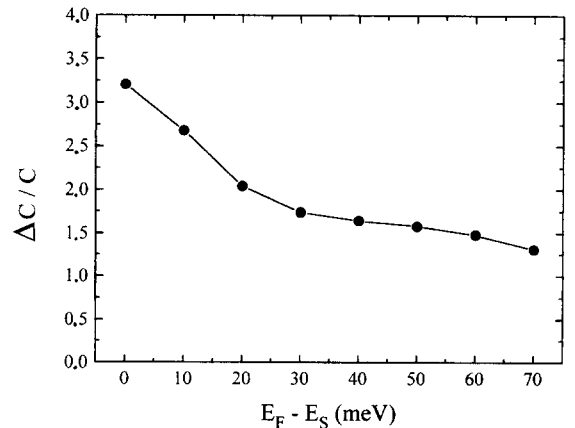


Fig. 9. Variation of the jump in the specific heat at $T = T_c$, $\Delta C/C$, versus the doping $D = E_F - E_s$.

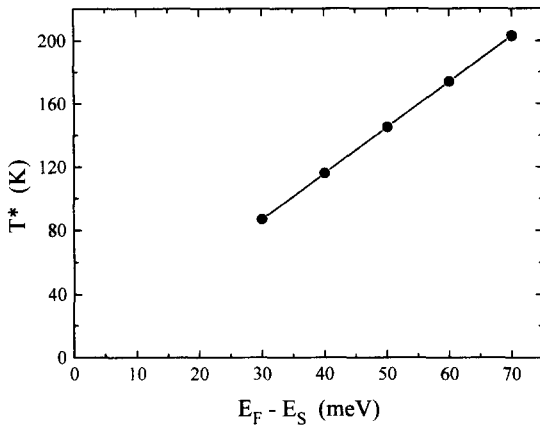


Fig. 10. Variation of the temperature T^* , where the change of behaviour of γ_N occurs, versus the doping $D = E_F - E_s$. T^* (meV) = 0.25D (meV) or T^* (K) = 2.9D (meV).

by Bok and Labbé in 1987 [18]. The specific heat $C_N(T)$ explores a domain of width $k_B T$ around the Fermi level E_F . So for $D < k_B T_c$, the variation of γ_N above T_c is logarithmic as predicted by Bok and Labbé (BL) [18]. For $D > 30$ meV, at high temperature $T - T_c > D$, the BL law is observed, but for lower temperatures γ_N increases with T and passes through a maximum at T^* as shown in Fig. 10. We shall now analyze the experimental observations and show that such a behaviour has been seen.

4.2. Comparison with experiments

Many authors have measured the specific heat of high T_c cuprates [17,19–24]. But it is difficult to compare all these experimental results to a theoretical model for the following reasons.

(i) It is difficult to extract the electronic specific heat C_s from the measured total specific heat C_{sT} which contains many other contributions, the contribution of the lattice vibrations, the contribution of magnetic fluctuations at low temperature and that of impurities and defects.

(ii) The homogeneity and quality of the samples has also an influence on C_{sT} .

(iii) Near T_c , the fluctuations of the order parameter must also be taken into account. These fluctua-

tions are usually assumed to be symmetric around T_c [15,17,24].

Several techniques have been used to extract C_s (see above references): extraction of the non-metallic phonon spectrum (for instance $YBa_2Cu_3O_6$ for $YBa_2Cu_3O_7$) or with a theoretical model, or by suppressing superconductivity with a high magnetic field [24].

To compare our results on the effect of doping on C_s with experiments, we have chosen the family of the $Tl_2Ba_2CuO_{6+\delta}$, studied by Loram et al. [25], because they are overdoped samples, with only one CuO_2 plane. The family $YBa_2Cu_3O_{6+x}$ is underdoped for $x < 0.92$ and for $x > 0.92$ the chains become metallic and play an important role [26–29]. However, recent results by Loram et al. [30] on calcium doped YBCO, $Y_{0.8}Ca_{0.2}Ba_2Cu_3O_{7-\delta}$, which are overdoped two dimensional systems, show a very good agreement with our results.

The Bi2212 compound exists only near optimum doping and many experiments at low temperature give a law $C_s \approx T^2$ attributed to magnetic fluctuations [31–36].

In the $Tl_2Ba_2CuO_{6+\delta}$ compounds studied by Loram et al. [25] δ varies from 0 to 0.1 and T_c from 85 to 0 K, and in the $Y_{0.8}Ca_{0.2}Ba_2Cu_3O_{7-\delta}$ [30] compounds δ varies from 0.29 to 0.04 and T_c from 85 to 45 K. Because of the difficulty to extract exactly C_s from the experimental data, we will compare only the general features to our calculation. We see that the oxygen doping has a strong influence on T_c and all the superconducting properties, so we assume that its role is to increase the density of holes in the CuO_2 planes.

We compare our calculations with the results published in Fig. 9 of Ref. [25], and in Fig. 2(a) of Ref. [30]. We notice the displacement and the decrease of the jump in specific heat C_s with doping. The jump at T_c optimum, $\Delta C/C = \Delta\gamma/\gamma$ is 1.67 [25], and 1.60 [30] greater than the BCS value 1.41 for a metal with a constant density of states. We find theoretically this increase of $\Delta C/C$ which in our model is due to the logarithmic van Hove singularity. The symmetrical shape of the peak of C_s , at low doping level, is due to the critical fluctuations. A subtraction of these fluctuations [17,24] gives an asymmetrical shape. For high doping levels the classical BCS shape is found.

We find a correct value for the coefficient γ_N in the normal state, without adjustable parameter. In the normal state our formula

$$\rho(\epsilon) = \frac{N}{\pi^2 D} \ln \frac{D}{\epsilon - E_s}$$

gives 0.6 mJ/gat K² the experimental value with $N = 10\%$ of holes per Cu atom. In fact, T_c is maximum for N of the order of 15 to 20%, but it is already very satisfactory that our approach gives the measured value of γ_N within a factor 1.5. For $\delta = 0$, we find that γ_N is not constant but given by the logarithmic law [18]:

$$\gamma_N = a \ln \frac{1}{T} + b$$

with $a = 0.04$, $b = 0.08$ when γ_N is measured in mJ/gat K² and T in K.

When δ increases, the law changes, γ_N passes through a maximum for a value of T that we call T^* . This behaviour is clearly seen in the YBCuO_{6+x} family [25].

We explain the high value $\Delta C/C|_{T_c} = 2.5$ for $x = 0.92$ in the YBCO family, and we find the predicted variation of T^* with x (Fig. 10).

Our model, neglecting magnetic fluctuations gives an Arrhenius law for C_s at low temperature with a characteristic energy which is Δ_{\min} . We see that such a law is observed in YBaCuO_{6.92} and for Tl₂Ba₂CuO₆ at optimum doping.

In conclusion we interpret the main features of the measurements of C_s and C_N (or γ_s and γ_N), the high value of the jump $\Delta C/C$ at T_c for $\delta = 0$, the decrease of that jump with doping, the variation of γ_N with T as a function of doping, the variation of C_s as $\exp(-\Delta_{\min}/(k_B T))$ for YBCO and Tl-BaCuO. We also explain with that model the observed tunneling characteristics and their variation with doping. Finally we predict that the gap anisotropy is reduced when the doping is increased, such a behaviour has been observed [11].

Acknowledgements

We would like to thank G. Deutscher (University of Tel Aviv), and J.W. Loram (University of Cambridge) for helpful discussions. This work has been supported by DRET, under contract No. 94-070.

References

- [1] J. Labbé, J. Bok, Europhys. Lett. 3 (1987) 1225.
- [2] J. Bouvier, J. Bok, Physica C 249 (1995) 117.
- [3] J. Bok, J. Bouvier, Physica C 244 (1995) 357.
- [4] J. Bok, J. Bouvier, L. Force, Electronic structure and high T_c superconductivity: an itinerant electron approach, in: G. Deutscher, A. Revcolevschi (Eds.), Coherence Effects in HTc Superconductors, World Scientific, Singapore, 1996.
- [5] L. Force, J. Bok, Solid State Commun. 85 (11) (1993) 975.
- [6] T. Yokoya, A. Chainani, T. Takahashi, H. Katayama-Yoshida, M. Kasai, Y. Tokura, Physica C 263 (1996) 505.
- [7] J. Bok, J. Bouvier, Gap anisotropy and van Hove singularities in high T_c superconductors, in: SPIE 96's West Photonics, vol. 2696 (1996).
- [8] J. Bok, J. Bouvier, Physica C 274 (1997) 1.
- [9] P. Bourge, L.P. Regnault, Y. Sidis, C. Vettier, Phys. Rev. B 53 (1996) 876.
- [10] Koike et al., Physica C 159 (1989).
- [11] M. Onellion, R.J. Kelley, D.M. Poirier, C.G. Olson, C. Kendziora, Superconducting energy gap versus transition temperature in Bi₂Sr₂CaCu₂O_{8+x}, preprint.
- [12] R.J. Kelley, C. Quitmann, M. Onellion, H. Berger, P. Almeras, G. Margaritondo, Science 271 (1996) 1255.
- [13] C. Renner, O. Fischer, private communication.
- [14] O. Riou, Etude de monocristaux d'YBa₂Cu₃O_{6.92} par la mesure micro-calorimétrique, thèse, 19 janvier 1996.
- [15] O. Riou, M. Charalambous, P. Gandit, J. Chaussy, P. Lejay, W.N. Hardy, Disymmetry of critical exponents in YBCO, in: LT 21 proceedings, preprint to be published.
- [16] L.N. Bulaevski et al., Physica C 152 (1988) 1849.
- [17] E. Janod, C. Marcenat, C. Baraduc, A. Junod, R. Corlemczuk, G. Deutscher, J. Henry, Physica C 235-240 (1994) 1763.
- [18] J. Bok, J. Labbé, C.R. Acad. Sci. Paris 305 (1987) 555–557, série II.
- [19] J.W. Loram, K.A. Mirza, J.R. Cooper, W.Y. Liang, J.M. Wade, J. Supercond. 7 (1994).
- [20] M. Roulin, A. Junod, E. Walker, Physica C 260 (1996) 257.
- [21] M. Roulin, A. Junod, Physica C 259 (1996) 193.
- [22] N. Overend, M.A. Houson, I.D. Laurie, Physica C 235-240 (1994) 1769.
- [23] A. Mirmelstein, A. Junod, G. Triscone, K.Q. Wang, J. Muller, Physica C 248 (1995) 335.
- [24] C. Marcenat, R. Calemczuk, A. Carrington, Specific heat of cuprate superconductors near T_c , in: G. Deutscher, A. Revcolevschi (Eds.), Coherence Effects in HTc Superconductors, World Scientific, Singapore, 1996.
- [25] J.W. Loram, K.A. Mirza, J.M. Wade, J.R. Cooper, W.Y. Liang, Physica C 235-240 (1994) 134.
- [26] N.E. Phillips, J.P. Emerson, R.A. Fischer, J.E. Gordon, B.F. Woodfield, D.A. Wright, Physica C 235-240 (1994) 1737.
- [27] V. Breit, P. Schweiss, R. Hauff, H. Whühl, H. Claus, H. Rietschell, A. Erb, G. Müller-Vogt, Phys. Rev. B 52 (1995) R15727.
- [28] V.Z. Kresin, S.A. Wolf, Phys. Rev. B 46 (1992) 6458.
- [29] V.Z. Kresin, S.A. Wolf, G. Deutscher, Physica C 191 (1992) 9.

- [30] J.W. Loram, K.A. Mirza, J.R. Cooper, J.L. Tallon, in: Proceedings of M²S-HTSC-V, Feb 28–Mar 4, 1997, Beijing, China, to be published.
- [31] H. Kierspel, E. Kopanakis, B. Buchner, A. Freimuth, W. Schlabit, V.H.M. Duijn, N.T. Hien, A.A. Menovsky, J.J.M. Franse, *Physica C* 235-240 (1994) 1765.
- [32] A. Junod, K.Q. Wang, T.T. Sukamoto, B. Revaz, G. Triscone, E. Walker, J. Müller, *Physica C* 235-240 (1994) 1761.
- [33] Y. Yamada, T. Okamoto, U. Mizatani, I. Mirabayashi, *Physica C* 232 (1994) 269.
- [34] M.K. Yu, J.P. Franck, *Physica C* 235-240 (1994) 1757.
- [35] T. Sasaki, Y. Muto, T. Shishido, T. Sasaki, T. Kajitani, M. Furuyama, N. Kobayashi, T. Fukuda, *Physica C* 162-164 (1989) 504.
- [36] E.B. Nyeanchi, D.F. Brewer, T.E. Margreaves, A.L. Thomson, C. LiezMao, C. Zhao Jia, *Physica C* 235-240 (1994) 1755.